Inorganic Chemistry

Communication

pubs.acs.org/IC

The Role of Modulators in Controlling Layer Spacings in a Tritopic Linker Based Zirconium 2D Microporous Coordination Polymer

Jialiu Ma, Antek G. Wong-Foy, and Adam J. Matzger*

Department of Chemistry, Macromolecular Science and Engineering Program, University of Michigan, 930 North University Avenue, Ann Arbor, Michigan 48109-1055, United States

Supporting Information

ABSTRACT: A 2D zirconium-based microporous coordination polymer derived from the tritopic linker 1,3,5-(4-carboxylphenyl)benzene, UMCM-309a, has been synthesized. This noninterpenetrated material possesses a $Zr_6(\mu_3\text{-}O)_4(\mu_3\text{-}OH)_4(RCO_2)_6(OH)_6(H_2O)_6$ cluster with six hexagonal-planar-coordinated linkers. UMCM-309a is stable in an aqueous HCl solution for over 4 months. The use of different monocarboxylates as modulators leads to similar 2D structures with different layer spacings; moreover, removal of the modulator yields the parent UMCM-309a.

Coordination polymers have seen extensive development in the nearly 100 years since their first description.[1,2] The delineation of the design principles for porous solids with controlled structure took place a few decades ago through the work of Robson.[3] These materials suffered from a lack of porosity in the absence of guests, and in 1999, two fantastic examples of porous coordination polymers with permanent porosity were described, heralding the area of what is now commonly referred to as metal−organic frameworks (MOFs) or microporous coordination polymers (MCPs).[4,5] These early examples suffered from water sensitivity, but rapid advances led to porous materials with more hydrolytically stable metal clusters, broadening the potential applicability of these materials in a host of gas storage and separation applications. Stable Al- and Cr-based MCPs were more recently joined by those based on Zr, and now MCPs are proving to be excellent desiccants for humid gas streams.[6,7] With increased stability came poorer crystallinity, and indeed single crystals are unattainable for many of the newest water-stable MCPs, whereas traditional Zn- and Cu-based MCPs often readily form large single crystals.

Currently, most Zr MCPs are built with ditopic linkers. The first example, UiO-66, uses terephthalic acid as the linker.[8,9] The $Zr_6O_4(OH)_4(RCO_2)_{12}$ cluster in this material has been shown to be one common mode of assembly, and by changing the length of the ditopic linker, Zr MCPs with the same topology (**fcu** net) and Zr_6 cluster are typically achieved with different pore sizes and surface areas. Another common class of linkers used in Zr MCP construction is tetratopic linkers such as porphyrin-based tetracarboxylic acids. These linkers generate MCPs with different topologies. For example, in PCN-222(Fe),[10] the Zr MCP constructed based on Fe-TCPP [TCPP = tetrakis(4-carboxyphenyl)porphyrin] adopts a **csq-a** net, whereas the same linker geometry also results in PCN-224[11] with a **she** net and PCN-225[12] with a **sqc** net. The change in the linker geometry also affects the Zr_6 cluster (a summary of common Zr_6 clusters is shown in Figures 1 and S1 in the Supporting Information, SI). In the UiO series of MCPs, each Zr_6 cluster is nominally 12 connected to the linkers. In the cases of PCN-222(Fe), PCN-224, and PCN-225, the Zr_6 cluster is only 8-, 6-, and 6-connected, respectively. Whereas tritopic linkers are a common class of linkers in building Zn or Cu MCPs, they are rarely used in building Zr MCPs. Only three Zr MCPs are found in the literature based on a tritopic linker. MOF-808 is built from trimesic acid and adopts the **spn** net with an atypical 6-connected cluster.[7] A second example is based on 1,3,5-(4-carboxylphenyl)-benzene (H_3BTB), a more extended tritopic linker than trimesic acid that possesses the same geometry, and is interpenetrated as well as much less stable compared to other 3D Zr MCPs.[13] The most recent addition, PCN-777, is constructed from the 4,4′,4″-*s*-triazine-2,4,6-triyltribenzoate linker with a 6-connected Zr_6 cluster.[14]

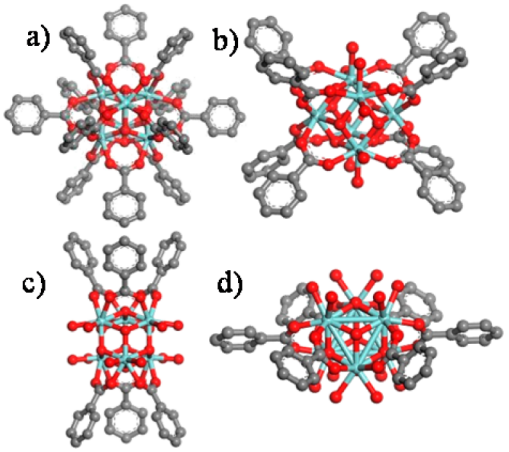

Figure 1. Summary of common Zr_6 clusters with different coordination numbers: (a) 12-coordinate; (b) 8-coordinate; (c) 6-coordinate (trigonal prismatic); (d) 6-coordinate (hexagonal planar).

Here we present a new Zr MCP, UMCM-309a, derived from the tritopic linker H_3BTB. Our first attempts to synthesize new materials using H_3BTB and $ZrCl_4$ resulted in amorphous products. This is a common issue encountered in Zr MCP chemistry. The use of modulators, such as monocarboxylic acid, has been applied to increase the crystallinity of Zr MCPs.[15] When

Received: February 19, 2015
Published: April 24, 2015

DOI: 10.1021/acs.inorgchem.5b00413
Inorg. Chem. 2015, 54, 4591−4593

added at sufficiently high concentrations, modulators slow crystal growth, affording increased crystallinity of the MCP.[16] By using concentrated HCl as the modulator, a crystalline phase was obtained (UMCM-309a). By using monocarboxylic acids as the modulator, including benzoic acid and biphenyl-4-carboxylic acid, the crystallinity of the product was further increased. However, suitable single crystals could not be obtained. These new phases (benzoic acid, UMCM-309b; biphenyl-4-carboxylic acid, UMCM-309c) are closely related to those arising from HCl, and the relationship among these materials is discussed below.

Without a suitable single crystal to determine the structure, we turn to the approach that was applied to find model structures for covalent organic frameworks. The general work flow is (a) index the PXRD pattern to determine the unit cell and crystal system, (b) determine the connectivity of the linker and cluster to find potential topologies in the Reticular Chemistry Structure Resource (RCSR),[17] ensuring that the topology is consistent with the geometry information of the cluster and linkers as well as indexing results, (c) build models based on the vertex information from the topology, and (d) optimize and refine the structure against the PXRD pattern.

When the PXRD pattern of UMCM-309a (material synthesized from HCl as the modulator) was indexed, the unit cell was determined to be hexagonal with $a=b = 20.06$ Å, $c = 7.07$ Å, $\alpha = \beta = 90°$, and $\gamma = 120°$. The very short c axis pointed to the likely involvement of a 2D-layered structure. BTB is 3-connected, whereas the Zr_6 cluster is commonly found to be 6-, 8-, 10-, or 12-connected. Theoretically possible topologies based on different connectivities of the vertices have been derived and compiled into the RCSR database. Searches based on 3, 6; 3, 8; 3, 10; and 3, 12 connectivity were conducted. Only **tfz-d** and **anh** nets and **bru** and **kgd** layers were found to be in the hexagonal group. The **tfz-d** and **anh** topologies were excluded because the geometry of the 8-connected unit is not compatible with the Zr_6 cluster shape. The **bru** topology was ruled out because it incorporates a pyramidal 3-connected unit that is not accessible for BTB. The **kgd** binodal 3,6-connected 2D kagome hexagonal net is consistent with indexing results and geometry information. The BTB linker and Zr_6 cluster were placed in the unit cell with cell parameters obtained from indexing in an arrangement consistent with the vertex information on the **kgd** topology. In fact, this topology is the same as the previously reported Zr/BTB phase,[13] although as shown below, the materials are distinct with regard to structure and reactivity. The model was geometry-optimized (Figure 2 and section 3 in the SI). A Pawley refinement was performed on the PXRD pattern to give the final cell parameters. The final refined unit cell for UMCM-309a is $a = b = 19.54 \pm 0.03$ Å, $c = 7.01 \pm 0.01$ Å, $\alpha = \beta = 90°$, $\gamma = 120°$, $R_p = 3.64\%$, and $R_{wp} = 5.81\%$ (Figure S2 in the SI).

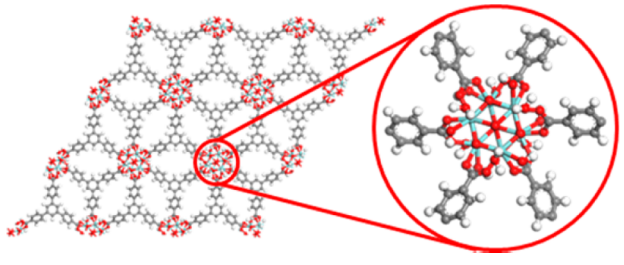

Figure 2. Model structure of UMCM-309a and expansion of a single Zr_6 cluster.

In the final structure for UMCM-309a (Figure 2), each cluster connects to six BTB ligands. The remaining sites are coordinated with six hydroxyl groups and six water molecules to give a neutral framework: $[Zr_6(\mu_3\text{-}O)_4(\mu_3\text{-}OH)_4(BTB)_2(OH)_6(H_2O)_6]$. This assignment is in reasonable accord with elemental analysis and TGA data (see details of formula in Section 2 and Figure S3 in SI) although the high carbon content suggests that residual BTB remains in the pores either as a guest or through coordination to the cluster (vide infra). A nitrogen isotherm was collected on this phase. A BET surface area of 810 m^2/g was obtained which is comparable to UiO-66 (Figure S4 in SI). The previously reported Zr/BTB phase, an interpenetrated version of the present material, has a BET surface area of 713 m^2/g.[19] The interpenetrated phase is claimed to have much lower stability compared to other 3D Zr MCPs. It is therefore surprising that UMCM-309a is found to be stable towards water and HCl solution for four months (Figure S7).

We now turn to the role of modulator. While modulators are extensively used in Zr MCP synthesis to increase crystallinity, they are often assumed to be removed from the framework after washing with polar solvents like *N*,*N*-dimethylformamide (DMF). However, it has been shown that modulators can function as defect sites in the framework or coordinate to the free sites of the cluster. In those cases, washing with DMF does not remove modulators coordinated to the cluster. Harsh conditions like treating MCPs with HCl in DMF at 120 °C help to remove all modulators. In such cases, removing modulators does not change the overall structure.[10,18] Presented here is a contrasting case where the modulator both plays a role in forming the structure and continues to exert influence upon removal.

When monocarboxylate modulators were examined (benzoic acid and biphenyl-4-carboxylic acid), a dramatic change in the PXRD patterns was observed compared to that of UMCM-309a, indicating a change in the overall structure. Attempts to activate these phases through solvent exchange and supercritical CO_2 activation[19,20] generated nonporous materials in contrast to the porous UMCM-309a. It was found that the new phases are not stable in air and the PXRD patterns changed upon solvent loss albeit with retention of the two main peaks with peak positions corresponding to the (1, 0, 0) and (1, 1, 0) reflections (Figure S11 in the SI). This suggests that the layered structure is still intact after the structure change. Thus, it was hypothesized that the changes arising in the PXRD pattern are attributable to a change in the distance between the layers (c axis). UMCM-309a possesses free hydroxyl sites that potentially can be substituted by monocarboxylic acid. Unlike more typical cases where the pillar linkers covalently bridge between layers in pillar-layered MCPs such as D-MOF[21] and UMCM-10, -11, and -12,[22] here monocarboxylic acid only coordinates to one layer, leading to weak interaction between layers. This then results in a structural change (collapse) specifically with regard to the distance between layers. NMR of the digested products using benzoic acid (UMCM-309b) and biphenyl-4-carboxylic acid (UMCM-309c) was performed, and the ratio between the modulator and BTB was determined to be close to 6:2, which implies that each cluster coordinates to six modulators (Figures S8 and S9 in the SI). Furthermore, before and after solvent removal, the ratio does not change. The hypothesis that the modulators change the c axis is further supported by analysis of the PXRD pattern. Considering the increase in the c axis when modulators are coordinated to the free sites, new peaks related to the c axis should emerge at lower 2θ angles. The PXRD pattern of UMCM-309c displays a new peak at $2\theta = 5.9°$, which is assigned as (0, 0,

DOI: 10.1021/acs.inorgchem.5b00413
Inorg. Chem. 2015, 54, 4591−4593

1), and related peaks, including (1, 0, 1), (1, 1, 1) and (2, 0, 1), can be found at the predicted positions based on the new unit cell parameters (Table S2 in the SI). A preliminary model was generated for UMCM-309c, and in this model, the free hydroxyl sites are replaced by biphenyl-4-carboxylic acid, resulting in a longer *c* axis (14.8 Å) compared to 7.04 Å of UMCM-309a. The model was refined against the PXRD pattern, giving fairly good agreement (Figure 3). Washing UMCM-309c with DMF several

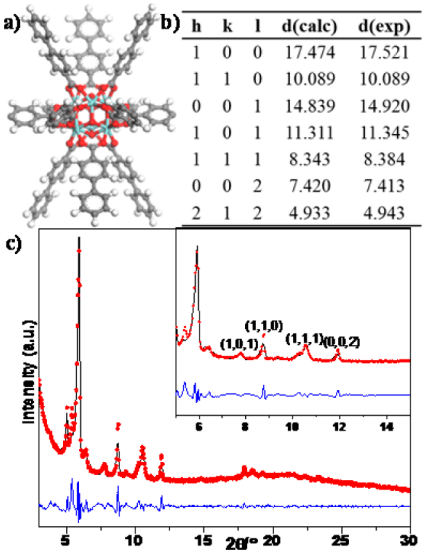

h	k	l	d(calc)	d(exp)
1	0	0	17.474	17.521
1	1	0	10.089	10.089
0	0	1	14.839	14.920
1	0	1	11.311	11.345
1	1	1	8.343	8.384
0	0	2	7.420	7.413
2	1	2	4.933	4.943

Figure 3. (a) Biphenyl-4-carboxylate coordinated to the free sites of the Zr_6 cluster. (b) Experimental and calculated peak positions of UMCM-309c based on a *c* axis of 14.8 Å. (c) Results of Pawley refinement for UMCM-309c.

times at room temperature did not change the ratio between the modulator and BTB. These modulators can be removed when UMCM-309c (or UMCM-309b) is treated in a DMF/H_2O (or DMF/HCl) mixture at 120 °C. The PXRD pattern changes to that of UMCM-309a (Figure S13 in the SI). The sharper peaks in the pattern indicate a more crystalline phase than that previously obtained. After treatment and activation at 120 °C under vacuum, the MCP shows a surface area of around 788 m^2/g, a value closely matching that of UMCM-309a and consistent with complete conversion of UMCM-309c upon modulator removal (Figure S14 in the SI). The modulator clearly plays more than a fleeting role in forming the structure here. In the case of benzoic acid, perhaps the most commonly used modulator in Zr MCP synthesis, a more complex structure than the other two phases is obtained. This may arise from partial collapse or a more profound structural change than that described above. However, here too the modulator is far from a spectator and instead is involved intimately in the resultant structure.

In this Communication, we report the synthesis and characterization of Zr MCP based on a tritopic linker (H_3BTB). It possesses a 2D layer structure with a short *c* axis. This porous phase is stable in aqueous conditions for over 4 months. The influence of using different modulators on the structure was also investigated, and in contrast to conventional cases, the modulators benzoic acid and biphenyl-4-carboxylic acid remain coordinated to the cluster. Clearly, more attention needs to be focused on the role of the modulator to ensure correct interpretation of the structural results, and the ability of the modulator to yield novel structures represents an emerging synthetic strategy.

■ ASSOCIATED CONTENT

Ⓢ Supporting Information

Synthetic procedures and characterization. This material is available free of charge via the Internet at http://pubs.acs.org.

■ AUTHOR INFORMATION

Corresponding Author

*E-mail: matzger@umich.edu.

Notes

The authors declare no competing financial interest.

■ ACKNOWLEDGMENTS

This work was supported by the Department of Energy (Award DE-SC0004888).

■ REFERENCES

(1) Shibata, Y. *J. Coll. Sci., Imp. Univ. Tokyo* **1916**, *37*, 1−36.
(2) Batten, S. R.; Champness, N. R.; Chen, X.-M.; Garcia-Martinez, J.; Kitagawa, S.; Ohrstrom, L.; O'Keeffe, M.; Suh, M. P.; Reedijk, J. *CrystEngComm* **2012**, *14*, 3001.
(3) Hoskins, B. F.; Robson, R. *J. Am. Chem. Soc.* **1989**, *111*, 5962.
(4) Li, H.; Eddaoudi, M.; O'Keeffe, M.; Yaghi, O. M. *Nature* **1999**, *402*, 276.
(5) Chui, S. S.-Y.; Lo, S. M.-F.; Charmant, J. P. H.; Orpen, A. G.; Williams, I. D. *Science* **1999**, *283*, 1148.
(6) Guo, P.; Wong-Foy, A. G.; Matzger, A. J. *Langmuir* **2014**, *30*, 1921.
(7) Furukawa, H.; Gándara, F.; Zhang, Y.-B.; Jiang, J.; Queen, W. L.; Hudson, M. R.; Yaghi, O. M. *J. Am. Chem. Soc.* **2014**, *136*, 4369.
(8) Cavka, J. H.; Jakobsen, S.; Olsbye, U.; Guillou, N.; Lamberti, C.; Bordiga, S.; Lillerud, K. P. *J. Am. Chem. Soc.* **2008**, *130*, 13850.
(9) Øien, S.; Wragg, D.; Reinsch, H.; Svelle, S.; Bordiga, S.; Lamberti, C.; Lillerud, K. P. *Cryst. Growth Des.* **2014**, *14*, 5370.
(10) Feng, D.; Gu, Z.-Y.; Li, J.-R.; Jiang, H.-L.; Wei, Z.; Zhou, H.-C. *Angew. Chem., Int. Ed.* **2012**, *51*, 10307.
(11) Feng, D.; Chung, W.-C.; Wei, Z.; Gu, Z.-Y.; Jiang, H.-L.; Chen, Y.-P.; Darensbourg, D. J.; Zhou, H.-C. *J. Am. Chem. Soc.* **2013**, *135*, 17105.
(12) Jiang, H.-L.; Feng, D.; Wang, K.; Gu, Z.-Y.; Wei, Z.; Chen, Y.-P.; Zhou, H.-C. *J. Am. Chem. Soc.* **2013**, *135*, 13934.
(13) Wang, R.; Wang, Z.; Xu, Y.; Dai, F.; Zhang, L.; Sun, D. *Inorg. Chem.* **2014**, *53*, 7086.
(14) Feng, D.; Wang, K.; Su, J.; Liu, T.-F.; Park, J.; Wei, Z.; Bosch, M.; Yakovenko, A.; Zou, X.; Zhou, H.-C. *Angew. Chem., Int. Ed.* **2015**, *54*, 149.
(15) Schaate, A.; Roy, P.; Godt, A.; Lippke, J.; Waltz, F.; Wiebcke, M.; Behrens, P. *Chem.—Eur. J.* **2011**, *17*, 6643.
(16) Wu, H.; Chua, Y. S.; Krungleviciute, V.; Tyagi, M.; Chen, P.; Yildirim, T.; Zhou, W. *J. Am. Chem. Soc.* **2013**, *135*, 10525.
(17) O'Keeffe, M.; Peskov, M. A.; Ramsden, S. J.; Yaghi, O. M. *Acc. Chem. Res.* **2008**, *41*, 1782.
(18) Deria, P.; Mondloch, J. E.; Tylianakis, E.; Ghosh, P.; Bury, W.; Snurr, R. Q.; Hupp, J. T.; Farha, O. K. *J. Am. Chem. Soc.* **2013**, *135*, 16801.
(19) Liu, B.; Wong-Foy, A. G.; Matzger, A. J. *Chem. Commun.* **2013**, *49*, 1419.
(20) Nelson, A. P.; Farha, O. K.; Mulfort, K. L.; Hupp, J. T. *J. Am. Chem. Soc.* **2008**, *131*, 458.
(21) Dybtsev, D. N.; Chun, H.; Kim, K. *Angew. Chem., Int. Ed.* **2004**, *43*, 5033.
(22) Dutta, A.; Wong-Foy, A. G.; Matzger, A. J. *Chem. Sci.* **2014**, *5*, 3729.

DOI: 10.1021/acs.inorgchem.5b00413
Inorg. Chem. 2015, 54, 4591−4593